Available online at www.sciencedirect.com

ScienceDirect

Ceramics International 40 (2014) 1073–1080

CERAMICS INTERNATIONAL

www.elsevier.com/locate/ceramint

# Synthesis and microwave dielectric properties of $Zn_2SnO_4$ ceramics

Qing Ma[a], Songping Wu[a,*], Yingxian Fan[b]

[a]School of Chemistry and Chemical Engineering, South China University of Technology, Guangzhou 510641, China
[b]Shen Zhen Zhen Hua Ferrite and Ceramic Electronics Co., Ltd., Shenzhen 518109, China

Received 19 April 2013; received in revised form 16 June 2013; accepted 28 June 2013
Available online 13 July 2013

**Abstract**

$Zn_2SnO_4$ ceramics were synthesized by the solid-state method. $B_2O_3$ was added into the system to lower the sintering temperature. $B_2O_3$-doped $Zn_2SnO_4$ materials were characterized by X-ray diffraction (XRD), electron microscopies (SEM/TEM/HRTEM/EDS), Raman and XPS spectroscopies. The inverse-spinel $Zn_2SnO_4$ ceramics (containing 1 wt% $B_2O_3$) sintered at 975 °C exhibited good microwave dielectric properties: $\varepsilon_r=9.3$, $Q\times f=62{,}000$ GHz and $\tau_f=-50$ ppm/°C. $Zn_2SnO_4$ ceramics with low sintering temperatures are promising candidate materials for low-temperature cofired millimeter-wave devices.


*Keywords:* Spinels; Dielectric materials/properties; Microstructure; Zinc oxide; Stannates

## 1. Introduction

In the last decade, the applications of microwave dielectric ceramics in the mobile communication system, intelligent transport system and microwave-integrated circuits have tremendously increased [1–3]. These materials used in microwave devices need a low dielectric constant ($\varepsilon_r$) to minimize the cross-coupling effect with conducts, a high quality factor ($Q\times f$) to increase their selectivity, and a near zero temperature coefficient of resonance frequency ($\tau_f$) value to ensure the stability of the frequency against temperature changes.

Several ceramic materials with low $\varepsilon_r$ and high $Q\times f$ value were reported, such as $Al_2O_3$ [4], $Sm_3Ga_5O_{12}$ [5], $Mg_4Nb_2O_9$ [6], $Mg_2SiO_4$ [7], $Zn_2SiO_4$ [8], $Ca_3SnSi_2O_9$ [9(a)], $CaSiSnO_5$ [9(b)], $RE_2SiO_5$ (RE=Sm [10(a)], Nd [10(b)]) and spinel $MAl_2O_4$ (M=Zn [11(a)], Mg [11(b)]). High performance microwave dielectric spinel $MAl_2O_4$ (M=Zn, Mg) ceramics have attracted much scientific and commercial attention owing to a single process and low cost.

Surendran et al. [11(a)] studied the microwave dielectric properties of the $ZnAl_2O_4$ and $MgAl_2O_4$ ceramics and found that $MgAl_2O_4$ exhibited following dielectric properties: $\varepsilon_r=8.8$, $Q\times f=68{,}900$ GHz and $\tau_f=-75$ ppm/°C. $ZnAl_2O_4$ ceramics sintered at 1650 °C possessed a low $\varepsilon_r$ value of 8.5, a high $Q\times f$ of 106,000 GHz, and a large negative $\tau_f$ value of −63 ppm/°C [11(a)]. Spinels could be proposed as excellent microwave substrate material; however, it is difficult to form dense structure for $MgAl_2O_4$ and $ZnAl_2O_4$ ceramics. The high sintering temperature (1650 °C) and a large negative $\tau_f$ value (~ −70 ppm/°C) have limited the application of spinels. Many works have been carried out to reduce the sintering temperatures and adjust $\tau_f$ values of spinel ceramics.

Adjustment of $\tau_f$ value could be achieved by adding other compounds having opposite $\tau_f$ value according to the dielectric mixing rule [11–14]. Rutile $TiO_2$ ceramics were usually employed to tune the $\tau_f$ value of ceramics with negative $\tau_f$ value because of their positive $\tau_f$ values. As reported in the literature [12], $0.83ZnAl_2O_4$–$0.17TiO_2$ and $0.79ZnAl_2O_4$–$0.21TiO_2$ (1500 °C) composite ceramics got near-zero $\tau_f$ value; however, the existence of second phase and abnormal microstructure were inevitable. When $ZnAl_2O_4$ mixed together with inverse-spinel structure ceramic $M_2TiO_4$ (M=Co, Mg and Mn), a solid solution should be formed because of their identical structures and similar ion radius, thus $M_2TiO_4$ could improve the sinterability of $ZnAl_2O_4$. For example, a fine

*Corresponding author.
*E-mail address:* chwsp@scut.edu.cn (S. Wu).

0272-8842/$ - see front matter © 2013 Elsevier Ltd and Techna Group S.r.l. All rights reserved.
http://dx.doi.org/10.1016/j.ceramint.2013.06.106

combination of dielectric properties ($\varepsilon_r$=9.9, $Q\times f$=94,000 GHz, $\tau_f$=−66.4 ppm/°C) could be achieved for the $0.79ZnAl_2O_4$–$0.21Co_2TiO_4$ solid solution [13]. Huang [14] and Lei [12] tried to adjust microwave dielectric properties of spinel through forming the solid solution and adding $TiO_2$. The influences of $ZnB_2O_4$ and $B_2O_3$ on the sintering characteristic of $(1-x)(0.79ZnAl_2O_4–0.21Co_2TiO_4)-xCaTiO_3$ ($x$=0.08) (ZCC) ceramics had been studied [15]. When $B_2O_3$ was added to ZCC system, the sintering temperature could reduce 50–100 °C. In our other studies, $B_2O_3$ was successfully employed to lower the sintering temperatures of $Mg_2GeO_4$ [16] and $ZnTiO_3$ ceramics [17].

Even though many researches have carried out on spinels, there still exists some problems for $MAl_2O_4$ (M=Zn, Mg) ceramics: (1) high sintering temperatures (≧1450 °C), second phase, and the complicated technology [11,12,14]; (2) the controversial dielectric response mechanism. Obviously, problems in $MAl_2O_4$ (M=Zn, Mg) ceramics are fundamental, so it is a vital issue to develop a novel spinel-based ceramics materials with low sintering temperature, high $Q\times f$ value and near-zero $\tau_f$ value.

$M_2SnO_4$ (M=Zn, Mg) ceramics were with inverse-spinel structure. $Mg_2SnO_4$ ceramics sintered at 1550 °C for 4 h had a dielectric constant of 8.41, a $Q\times f$ of 55,100 GHz and a $\tau_f$ value of −62 ppm/°C, and were potential candidates for millimeter wave application [18]. $(Mg_{0.93}Co_{0.07})_2SnO_4$ ceramics sintered at 1550 °C for 4 h had a dielectric constant of 8.9, a $Q\times f$ of 110,800 GHz (at 16.4 GHz) and a $\tau_f$ of −66 ppm/°C [19]. $Zn_2SnO_4$ was first prepared by Coffeen with the wet method and considered as an oxide semiconductor [20]. Its crystal structure was determined to be inverse spinel structure with the space group of *Fd*3*m* [21]. However, dielectric applications of inverse-spinel $Zn_2SnO_4$ ceramics have not been investigated yet. In this work, microwave dielectric properties of $Zn_2SnO_4$ ceramic were studied, and the relation between structures and properties of $Zn_2SnO_4$ ceramics has also been revealed.

## 2. Experimental procedure

The samples were prepared by the conventional solid-state method. ZnO (AR, Shantou, Guangdong), and nano-$SnO_2$ (99%, Aladdin, Shanghai, China) powders were mixed with a stoichiometric molar ratio in $Zn_2SnO_4$, and then milled with zirconia balls and deionized water for 4 h on a planetary milling machine (QM-3SP2, Zhenguang, Nanjing, China) to get mixtures. After drying at 100 °C for 24 h, these mixtures were partially pressed into green bodies of 10 mm diameter and 2 mm thickness with a manually tableting machine (769YP, Tianjin, China) under 8 MPa pressure. The green bodies were sintered at low temperatures (600–1000 °C) with a high-temperature electric furnace (SSJ-1600, Shenjia kiln, Luoyang, China) to obtain the low-temperature bulk ceramics for behavior research.

The mixtures were calcined at 1000 °C to produce $Zn_2SnO_4$ powders, which were re-milled for 4 h with 1–3 wt% $B_2O_3$ (≧99% purity) and dried. The re-milled powders were pressed into cylindrical disks of 10 mm diameter and about 6 mm thickness under about 10 MPa pressure isostatically using 5 wt % polyvinyl alcohol (PVA) organic binder as binder. These pellets were preheated 580 °C for 2 h to expel the binder and then sintered at 875–1000 °C for 4 h in air to obtain ceramics.

The crystalline phases of the $Zn_2SnO_4$ specimens were identified by X-ray diffraction (D8 ADVANCE, Bruker, Germany) using Cu Ka ($\lambda$=0.15406 nm) radiation with a graphite monochromator in the $2\theta$ range of 10–80° operated at 30 kV and 30 mA. The cell parameters were refined with software Jade 6.0. Transmission electron microscopy (TEM), high-resolution TEM (HRTEM) images and selected area electron diffraction (SAED) pattern were taken by a JEM-2100 electron microscopy (JEM-2100, JEOL, Tokyo, Japan) with an accelerating voltage of 200 kV. Element analysis of microdomain was carried out with an energy dispersive spectrometer (EDS) (EPMA1600, Shimadzu, Japan). Raman spectra of $Zn_2SnO_4$ powders and the polished and thermally etched ceramic surfaces were obtained with Micro-Raman spectrometer (LabRAM Aramis, HJY, France). Composition and chemical states of surface elements of $Zn_2SnO_4$ particles were investigated by XPS (Kratos Axis Ultra DLD, Japan) using Al Ka as exciting X-ray source. The spectra was calibrated with respect to the C 1s peak resulted from the adventitious hydrocarbon at the energy of 282.5 eV. The microstructure observations of $Zn_2SnO_4$ ceramics were performed under a scanning electron microscope (SEM) (LEO 1530 VP; Zeiss, Vertrieb Deutschland, Germany). The bulk densities of ceramics were measured by the Archimedes' method. Dielectric constants ($\varepsilon_r$) and the quality factor ($Q\times f$) values at microwave frequencies were measured by Hakki and Coleman [22] dielectric resonator method using a Network Analyzer (N5230 PNA-L, Agilent, Santa Clara, USA). Temperature coefficient of resonant frequency ($\tau_f$) was also measured by the same method with a changing temperature from 25 °C to 75 °C, and was calculated by the following equation:

$$\tau_f = \frac{f_{75}-f_{25}}{f_{25}\times 50}\times 10^6 \quad (1)$$

where $f_{75}$ and $f_{25}$ represent the resonant frequency at 75 °C and 25 °C, respectively.

## 3. Results and discussion

### 3.1. Phase identification of $Zn_2SnO_4$ ceramics

The XRD patterns of $Zn_2SnO_4$ low-temperature ceramics (molar ratio of $ZnO/SnO_2$=2) sintered at 800–1000 °C for 4 h are shown in Fig. 1. When the green bodies were sintered under the temperatures of 800–900 °C, the main crystal phases of specimens were ZnO (JCPDS no. 36-1457) and $SnO_2$ (JCPDS no. 41-1445). As the sintering temperature increased to 950 °C, $Zn_2SnO_4$ (JCPDS no. 24-1470) with space group *Fd*-3*m* (227) appeared. A single phase $Zn_2SnO_4$ occurred at 1000 °C, suggesting complete reaction between ZnO and $SnO_2$.

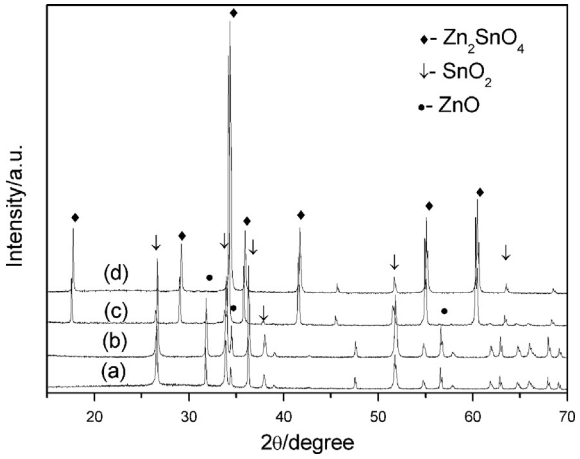


Fig. 1. X-ray diffraction patterns of ZnO–$SnO_2$ low-temperature ceramics sintered at various temperatures: (a) 800 °C, (b) 900 °C, (c) 950 °C, (d)1000 °C for 4 h.

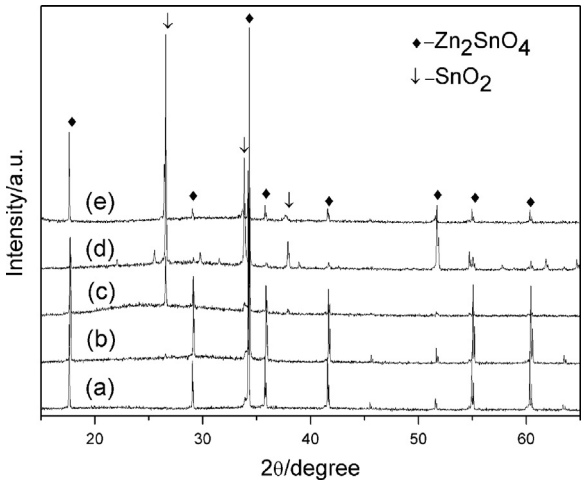


Fig. 2. X-ray diffraction patterns of $Zn_2SnO_4$ ceramics sintered at various temperatures: (a) 1100 °C, (b) 1150 °C, (c) 1200 °C, (d) 1250 °C, (e) 1300 °C for 4 h.

The XRD patterns of $Zn_2SnO_4$ ceramics sintered at 1100–1300 °C for 4 h are shown in Fig. 2, which suggested the formation of a single-phase cubic structure below 1150 °C. The lattice parameters were calculated as $a=b=c=8.657$ Å with the Jade 6.0 software. When sintered at above 1200 °C, the $SnO_2$ secondary phase was detected. Clearly, zinc tin oxide ($Zn_2SnO_4$) was the main crystalline phase, accompanied with small amounts of $SnO_2$. The content of $SnO_2$ increased with increasing temperatures.

Although the solid-state route is inexpensive and simple, there are some difficulties to prepare the single phase of $Zn_2SnO_4$ because of the existence of $SnO_2$ and the evaporation of ZnO [23]. Microwave dielectric properties of $Zn_2SnO_4$ (sintered at 1100 °C) were: $\varepsilon_r=8.16$, $Q\times f=19{,}070$ GHz (14.84 GHz) owing to the low relative density, thus it is very important to get dense $Zn_2SnO_4$ ceramics at low sintering temperatures. In this study, $B_2O_3$ was employed to reduce the sintering temperatures.

### 3.2. $B_2O_3$ doped $Zn_2SnO_4$ ceramics

#### 3.2.1. Phase identification of $B_2O_3$ doped $Zn_2SnO_4$ ceramics

Fig. 3(1) shows the XRD patterns of the $Zn_2SnO_4$+$x$ wt% $B_2O_3$ ceramics ($x=1$, 2 and 3) sintered at 950 °C for 4 h. All samples exhibited single phase, and their diffraction peaks could be indexed according to the cubic structure $Zn_2SnO_4$. Fig. 3(2) showed the XRD patterns of 1 wt% $B_2O_3$ doped $Zn_2SnO_4$ (assigned as $Z_2B_1$) sintered at different temperatures. The $Z_2B_1$ sample sintered at 975 °C possessed much better crystallinity, implying that their grain crystallinity depended on the sintering temperatures significantly. The strengths of (511) and (440) reflection were almost invisible for the specimens sintered at 1000 °C. It could be ascribed to the existence of the oriented growth in the ceramic surface, which resulted in lattice distortion.

#### 3.2.2. HRTEM studies

Fig. 4(a–d) showed the sample consisted of nanoplates with a width of 100–200 nm and the length 400–500 nm. Further insight on the monocrystal was gained by HRTEM observation on the edge area (presented by A) of the plate, as indicated in Fig. 4(a). They displayed distinct lattice spacings of 0.502, 0.261 nm and 0.304 nm, corresponding to a distance of (111), (311) and (220) lattice planes, respectively. Obvious screw dislocation could be observed (presented by the circle) in Fig. 4 (b). It showed the growth of $Zn_2SnO_4$ crystal followed the screw dislocation growth mechanism [24]. The corresponding SAED pattern Fig. 4(c) showed the presence of sharp diffraction spots, indicating that the $Zn_2SnO_4$ grains have good crystallinity and possess single crystalline structures. To confirm the chemical composition of these samples, energy dispersive X-ray spectroscopy (EDS) spectra (Fig. 4(d)) taken at a number of selected positions of the sample, showing that the expected presence of Zn, Sn, and O; and the atomic ratio of Zn:Sn was 2:0.93. The results clearly displayed the grains were Sn-deficient $Zn_2SnO_4$,

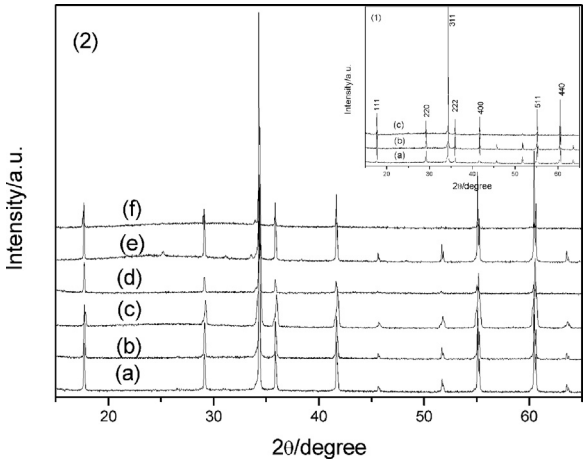


Fig. 3. (1) X-ray diffraction patterns of $Zn_2SnO_4$ (1–3 wt% $B_2O_3$) ceramics sintered at 950 °C:(a) $Z_2B_1$, (b) $Z_2B_2$, (c) $Z_2B_3$; (2) X-ray diffraction patterns of 1 wt% $B_2O_3$ doped $Zn_2SnO_4$ ceramics ($Z_2B_1$) sintered at various temperatures: (a) 875 °C, (b) 900 °C, (c) 925 °C, (d) 950 °C, (e) 975 °C, (f) 1000 °C for 4 h.

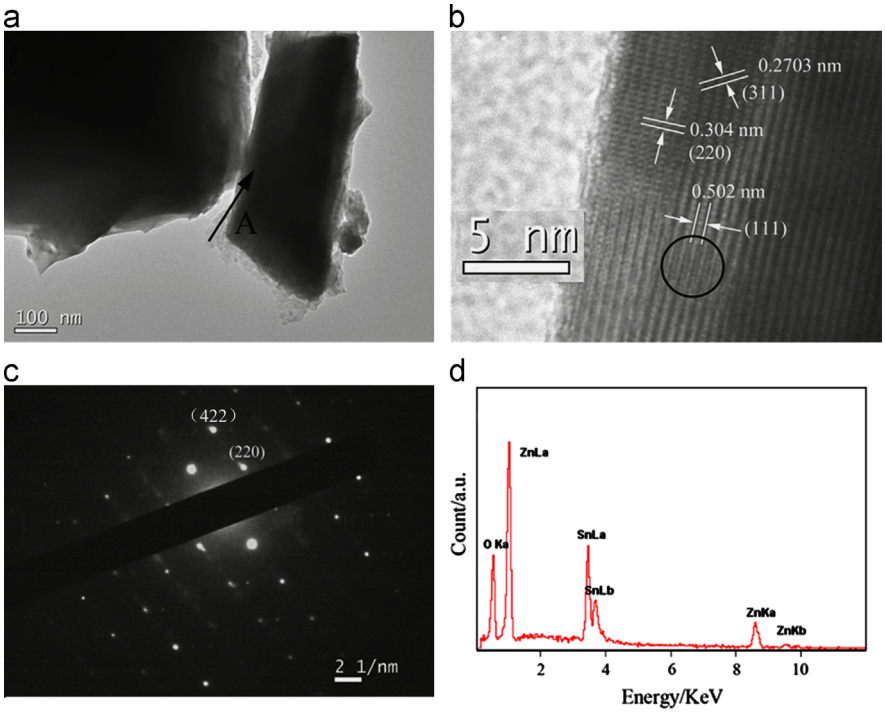


Fig. 4. (a) TEM image, (b) HRTEM image, (c) the selected electron diffraction pattern, (d) EDS pattern of $Zn_2SnO_4$ crystal calcined at 1100 °C.

which were also testified by the photoluminescence (PL) spectrum of the $Zn_2SnO_4$ nanowires [25–27].

### 3.2.3. Raman studies

$Zn_2SnO_4$ has a typical inverse spinel structure [19]. The schematic crystal structure is presented in Fig. 5(1). The Zn atom is centered at a $ZnO_4$ tetrahedron with four nearest-neighbor O atoms, while the same numbers of Zn and Sn atoms are at the center of octahedra with six nearest-neighbor O atoms. The O atoms are positioned in the same way in all octants with 5/2 Zn atoms and 3/2 Sn atoms as the nearest neighbors [28].

The local atomic structure of $Zn_2SnO_4$ powders calcined at 975 °C was characterized by Raman spectroscopy (see Fig. 5). Raman mode near 226.5 $cm^{-1}$ is quite weak, which may be caused by the overlapping effect with the laser-induced plasma [29]. The modes at 225.70, 375.66, 528.69, 552.50 and 670.26 $cm^{-1}$ can be reasonably assigned to $F_{2g}(1)$, $E_g$, $F_{2g}(2)$, $F_{2g}(3)$, and $A_{1g}$ symmetries. Raman peaks at about 528.7 and 670.2 $cm^{-1}$ are associated with stretching vibrations of short M–O bonds in the $MO_6$ octahedron sticking out into the structure spaces and internal vibrations of oxygen tetrahedron of $Zn_2SnO_4$, respectively [30].

### 3.2.4. XPS

XPS was further used to investigate the composition and surface electron state of $Z_2B_1$ ceramics sintered at 950 °C. Fig. 6 showed the XPS spectra of $Zn_2SnO_4$, and the whole scanning spectrum indicated the existing elements of Sn, Zn and O (Fig. 6(a)). The fine XPS spectrum, as displayed in Fig. 6(b), revealed Sn $3d_{3/2}$ and $3d_{5/2}$ peaks were at 492.2 eV and 483.8 eV, respectively. The result was agreeable to the reference value [31], indicating that the state of Sn was $Sn^{4+}$. The fine XPS spectrum (Fig. 6(c)) of Zn 2p peaks consisted of two peaks corresponding to 1018.7 eV and 1041.8 eV, which were caused by split of energy level because of spin–orbit coupling. The gap between the two peaks is 23.1 eV which was also consistent with the reference value of 23.0 eV [32]. The fine XPS spectrum of O 1s at 527.7 eV, which was agreeable to the reference value of 530.2 eV [33], is displayed in Fig. 6(d).

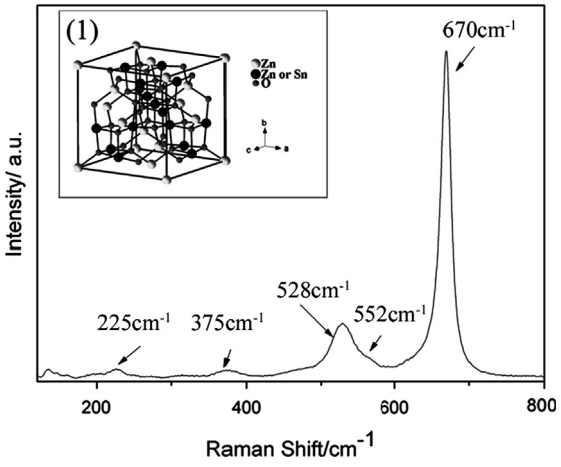


Fig. 5. Raman spectrum of $Zn_2SnO_4$–1 wt% $B_2O_3$ ceramics sintered at 975 °C and (1) the structure of $Zn_2SnO_4$.

### 3.2.5. SEM studies

SEM photographs of $B_2O_3$-doped $Zn_2SnO_4$ ceramics sintered at various temperatures are exhibited in Fig. 7. The $Zn_2SnO_4$ ceramics without $B_2O_3$ sintered at 1150 °C (as

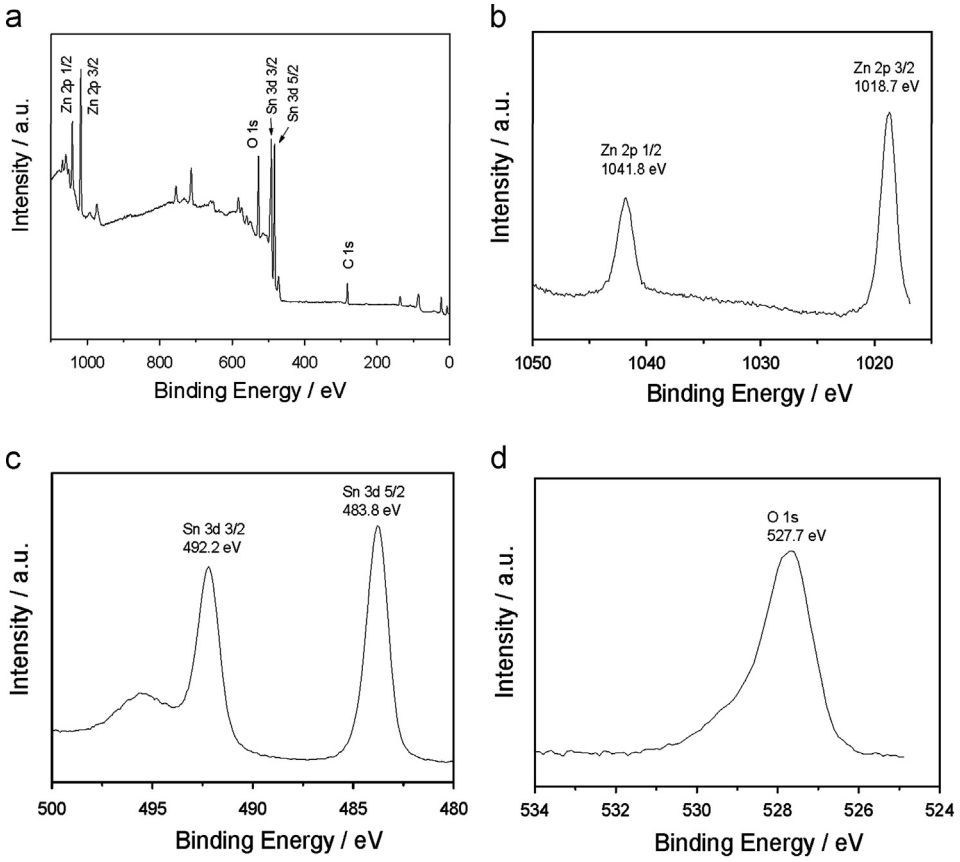


Fig. 6. XPS spectra of $Zn_2SnO_4$ particles calcined at 1100 °C: (a) whole scanning spectrum, the fine spectra of (b) Sn 3d, (c) Zn 2p and (d) O 1s.

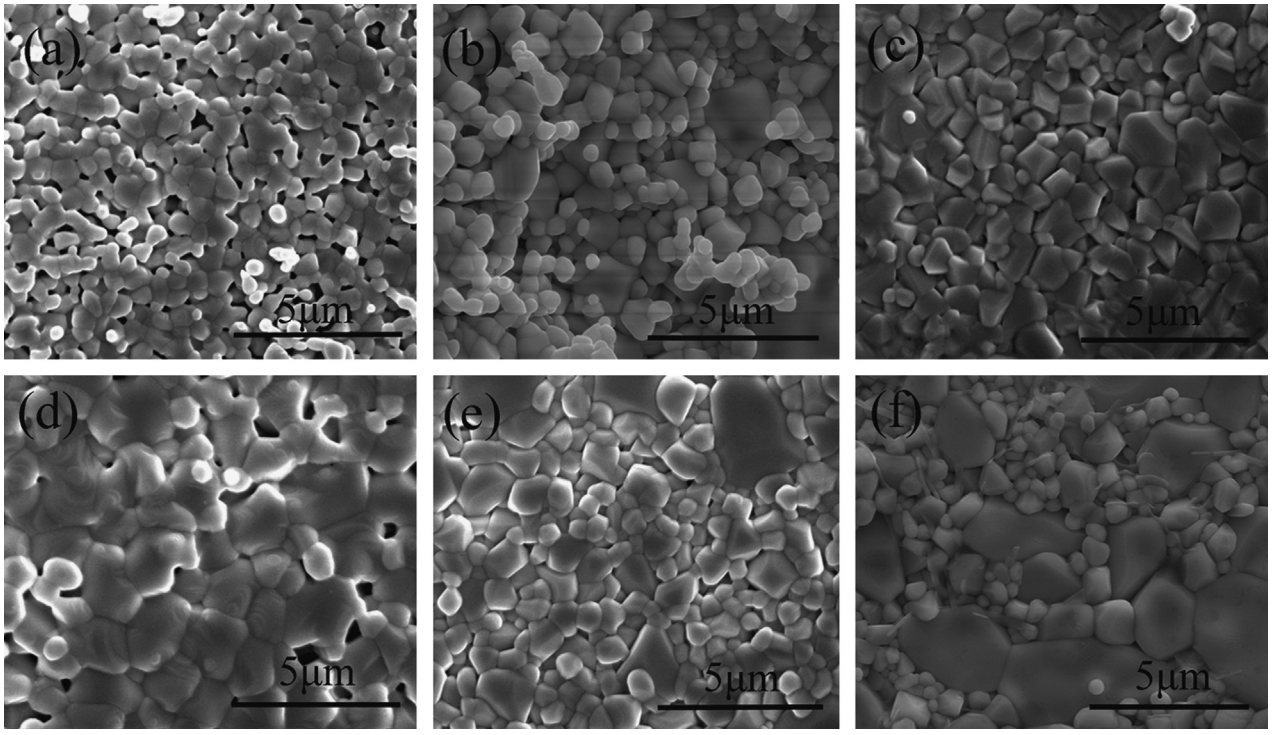


Fig. 7. SEM photographs of $Zn_2SnO_4$ ceramics sintered at various temperatures: (a) $Zn_2SnO_4$—1150 °C, (b, c and d) $Zn_2SnO_4$–1 wt% $B_2O_3$ sintered at 950, 975, and 1000 °C, respectively, (e) $Zn_2SnO_4$–2 wt% $B_2O_3$ and (f) $Zn_2SnO_4$–3 wt% $B_2O_3$ sintered 950 °C for 4 h.

shown in Fig. 7(a)) had a porous microstructure with an average grain size of 0.5–1 μm, which caused the low $Q \times f$ value. When $B_2O_3$ was added, the dense microstructure was developed and obvious grain growth occurred. The results indicated that $B_2O_3$ could effectively enhance the sintering of $Zn_2SnO_4$ ceramics.

Compared with different specimens with various amounts of $B_2O_3$ sintered at 950 °C, all the ceramics had few pores as shown in Fig. 7(b, e and f). Grain growth was promoted and dense structures were developed with increasing amounts of $B_2O_3$ due to the liquid phase. However, abnormal grain growth appeared when 3 wt% $B_2O_3$ was employed.

For $Zn_2SnO_4$ ceramics containing 1 wt% $B_2O_3$ (assigned as $Z_2B_1$) sintered at different temperatures, the average grain size increased as the sintering temperatures increased, as given in Fig. 7(b–d). When the sintering temperature was 1000 °C, a little of the liquid phase were found in the grain-boundaries. SEM micrograph of $Z_2B_1$ sintered at 975 °C indicated that the sample possessed better uniformity of grains and more compact microstructure (Fig. 7(c)).

### 3.2.6. Microwave dielectric properties

The relative densities and microwave dielectric properties of $Zn_2SnO_4-x$ wt% $B_2O_3$ ($x=1$, 2, 3) ceramics sintered at various temperatures for 4 h are summarized in Fig. 8. The relative density of $Zn_2SnO_4$ ceramics increased with the sintering temperatures increasing and reached the max value at 975 °C. The $Z_2B_1$ sintered at 975 °C showed a high relative density, approximately more than 96% of the theoretical density. The $\varepsilon_r$ value of $Z_2B_1$ ceramics sintered at 925 °C was 6.96, probably due to the low relative density and porous microstructures; however, it increased with temperatures increasing to a maximum value of 9.3 as sintered at 975 °C. The density and dielectric constant displayed the same trend with the sintering temperatures.

It was worth noting that the dielectric constant of $Zn_2SnO_4$ ceramics of 9.3 was more than that of $Mg_2SnO_4$ (8.41) [17]. It could be explained with the following Clausius–Mosotti equation:

$$\varepsilon_r = \frac{3}{1-b\alpha_m/V_m} - 2 \quad (2)$$

where $V$ is the molecular volume, $\alpha_m$ is dielectric polarizability, and $b=4\pi/3$. $Zn_2SnO_4$ and $Mg_2SnO_4$ are with the same crystal system and space group ($Fd$-3$m$ (227)), and their molecular volumes are 81.12 Å$^3$ and 80.55 Å$^3$, respectively. Because dielectric polarizability of $Zn^{2+}$ (2.04) is more than that of $Mg^{2+}$ (1.50) [34], the dielectric constant of $Zn_2SnO_4$ is larger than that of $Mg_2SnO_4$.

Generally, the $Q \times f$ value is affected by many factors such as lattice vibrational modes, pores, second phases, impurities, lattice defect, crystallizability, cation ordering, and inner stress. It is difficult to determine the key influential factor [35]. The $Q \times f$ value of $Z_2B_1$ ceramics increased to 62,000 GHz (sintered at 975 °C) from 15,700 GHz (sintered at 925 °C), as exhibited in Fig. 8(c). The increase in grain size probably produced a large $Q \times f$ value considering the high relative densities (about 96.5%) and uniform microstructure. With the increasing $B_2O_3$ content, the densification temperatures of $Zn_2SnO_4$ ceramics, corresponding to the max $Q \times f$ value,

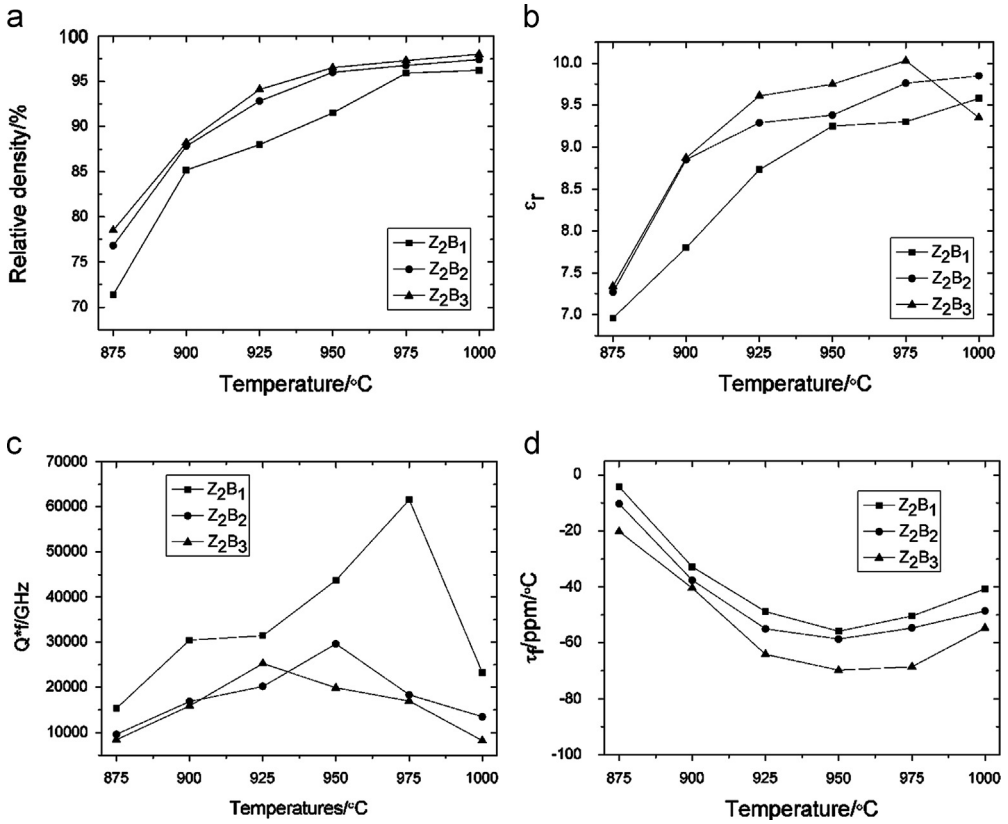


Fig. 8. (a) The relative densities, (b) $\varepsilon_r$, (c) $Q \times f$, and (d) $\tau_f$ values of $B_2O_3$-doped $Zn_2SnO_4$ ceramics sintered at various temperatures.

decreased. For example, the $Q \times f$ value of $Zn_2SnO_4$ ceramics containing 2 wt% $B_2O_3$ (assigned as $Z_2B_2$) decreased to 30,000 GHz (at 950 °C). The quality factor value changed to 25,000 GHz (at 925 °C) for $Zn_2SnO_4$ ceramics containing 3 wt % $B_2O_3$ (assigned as $Z_2B_3$). In addition, $Q \times f$ values decreased as the amount of $B_2O_3$ increased in the region of 950–1000 °C because of more impurity, abnormal grain growth and liquid-phase in grain boundaries.

The $\tau_f$ values of the $B_2O_3$-doped $Zn_2SnO_4$ ceramics sintered at various temperatures are shown in Fig. 8(d). $\tau_f$ values decreased as the sintering temperatures improved from 875 °C to 950 °C. The exact mechanism was not clear yet. A possible reason was the increase in cation ordering with the sintering temperature increasing [36]. For the $Z_2B_1$ ceramics, samples sintered at 975 °C exhibited the good microwave dielectric properties: $\varepsilon_r = 9.3$, $Q \times f = 62{,}000$ GHz and $\tau_f = -50$ ppm/°C.

Although the $Q \times f$ value of the $Zn_2SnO_4$ ceramics were lower than that of $MgSiO_3$ [37], $Mg_2SiO_4$ [7] or $Zn_2SiO_4$ [8] ceramics, it was comparable with the $Sm_2SiO_5$ [10(a)] or $CaSiSnO_5$ [9(b)] ceramics, and higher than that of $CaSiO_3$ [38], $Nd_2SiO_5$ [10(b)] or $Mg_2SnO_4$ [17] ceramics. Compared with conventional spinel-structured ceramic materials such as $MgAl_2O_4$ [11(b)], $ZnAl_2O_4$ [11(a)] and $ZnGa_2O_4$ [39], $B_2O_3$-doped $Zn_2SnO_4$ ceramics could be sintered at low temperature region (900–1000 °C), and considered as promising candidate materials for low-temperature cofired millimeter-wave devices.

## 4. Conclusions

Spinel $Zn_2SnO_4$ ceramics were synthesized using a solid-state method. The microstructure and microwave dielectric properties of the $Zn_2SnO_4$ ceramics were investigated to assess their potential application in low-temperature cofired millimeter-wave devices. ZnO and $SnO_2$ reacted to form single-phase cubic structure $Zn_2SnO_4$ (at 1000 °C), which decomposed at above 1200 °C. $B_2O_3$ was applied to lower the sintering temperatures of $Zn_2SnO_4$ ceramics. The large relative density, uniform grain growth, and dense microstructures resulted in high $Q \times f$ values. The $Zn_2SnO_4$ with 1 wt% $B_2O_3$ sintered at 975 °C exhibited the following microwave dielectric properties: $\varepsilon_r = 9.3$, $Q \times f = 62{,}000$ GHz and $\tau_f = -50$ ppm/°C.

## References


[1] C.L. Huang, K.H. Chiang, Characterization and dielectric behavior of CuO-doped $ZnTa_2O_6$ ceramics at microwave frequency, Materials Research Bulletin 39 (2004) 1701–1705.

[2] J.X. Tong, Q.L. Zhang, H. Yang, J.L. Zou, Low-temperature firing and microwave dielectric properties of $Ca[(Li_{0.33}Nb_{0.67})0.9Ti_{0.1}]O_{3-\delta}$ ceramics with LiF addition, Materials Letters 59 (2006) 3252–3254.

[3] A. Stiegelschmitt, A. Roosen, C. Ziegler, S. Martius, L.P. Schmidt, Dielectric data of ceramic substrates at high frequencies, Journal of the European Ceramic Society 24 (2004) 1463–1465.

[4] Y. Ohishli, Y. Miyauchi, H. Ohsato, et al., Control1ed temperature coefficient of resonant frequency of $A1_2O_3$–$TiO_2$ ceramics by annealing treatment, Japanese Journal of Applied Physics 43 (6A) (2004) L749–L751.

[5] J.C. Kim, M.H. Kim, S. Nahm, Microwave dielectric properties of $Re_3Ga_5O_{12}$ (Re: Nd, Sm, Eu, Dy and Yb) ceramics and effect of $TiO_2$ on the microwave dielectric properties of $Sm_3Ga_5O_{12}$ ceramics, Journal of the European Ceramic Society 27 (8–9) (2007) 2865–2870.

[6] S.W. Lim, J. Bang, Microwave dielectric properties of $Mg_4Nb_2O_9$ ceramics produced by hydrothermal synthesis, Journal of Electroceramics 23 (2–4) (2009) 116–120.

[7] K.X. Song, X.M. Chen, X.C. Fan, Effect of Mg/Si ratio on microwave dielectric characteristics of forsterite ceramics, Journal of the American Ceramic Society 90 (6) (2007) 1808–1811.

[8] M.Z. Dong, Z.X. Yue, Z. Zhuang, S.Q. Meng, L.T. Li, Microstructure and microwave dielectric properties of $TiO_2$-doped $Zn_2SiO_4$ ceramics synthesized through the sol–gel process, Journal of the American Ceramic Society 91 (12) (2008) 3981–3985.

[9] (a) S.P. Wu, D.F. Chen, Y.X. Mei, Q. Ma, Synthesis and microwave dielectric properties of $Ca_3SnSi_2O_9$ ceramics, Journal of Alloys and Compounds 521 (2012) 8–11;
(b) S.P. Wu, D.F. Chen, C. Jiang, Y.X. Mei, Q. Ma, Synthesis of monoclinic $CaSnSiO_5$ ceramics and their microwave dielectric properties, Materials Letters 91 (2013) 239–241.

[10] (a) S.P. Wu, C. Jiang, Y.X. Mei, W.P. Tu, Synthesis and microwave dielectric properties of $Sm_2SiO_5$ ceramics, Journal of the American Ceramic Society 95 (1) (2012) 37–40;
(b) C. Jiang, S.P. Wu, Q. Ma, Y.X. Mei, Synthesis and microwave dielectric properties of $Nd_2SiO_5$ ceramics, Journal of Alloys and Compounds 544 (2012) 141–144.

[11] (a) K.P. Surendran, N. Santha1, P. Mohanan, M.T. Sebastian, Temperature stable low loss ceramic dielectrics in $(1-x)ZnAl_2O_4-xTiO_2$ system for microwave substrate applications, European Physical Journal B 41 (2004) 301–306;
(b) K.P. Surendran, P.V. Bijumon, P. Mohanan, M.T. Sebastian, $(1-x)MgAl_2O_4-xTiO_2$ dielectrics for microwave and millimeter wave applications, Applied Physics A 81 (2005) 823–826.

[12] (a) W. Lei, W.Z. Lu, J.H. Zhu, X.H. Wang, Microwave dielectric properties of $ZnAl_2O_4$–$TiO_2$ spinel-based composites, Materials Letters 61 (2007) 4066–4069;
(b) W. Lei, W.Z. Lu, J.H. Zhu, X. Ye, Effects of heating rate on microwave dielectric properties of $(1-x)ZnAl_2O_4-xTiO_2$ ($x=0.21$) ceramics, Ceramics International 35 (2009) 277–280.

[13] C.W. Zheng, S.Y. Wu, X.M. Chen, K.X. Song, Modification of $MgAl_2O_4$ microwave dielectric ceramics by Zn substitution, Journal of the American Ceramic Society 90 (5) (2007) 1483–1486.

[14] C.L. Huang, T.J. Yang, C.C. Huang, Low dielectric loss ceramics in the $ZnAl_2O_4$–$TiO_2$ system as a $\tau_f$ compensator, Journal of the American Ceramic Society 92 (1) (2009) 119–124.

[15] W. Lei, Microstructures and properties of ZnAl2O4-based low-permittivity microwave dielectric ceramics, Huazhong University of Science and Technology 6 (2008) 100–105.

[16] C.X. Chen, S.P. Wu, J.H. Li, Synthesis and microwave dielectric properties of $B_2O_3$-doped $Mg_2GeO_4$ ceramics, Journal of Alloys and Compounds 578 (2013) 153–156.

[17] S.P. Wu, J.H. Luo, S.X. Cao, Microwave dielectric properties of $B_2O_3$-doped $ZnTiO_3$ ceramics made with sol–gel technique, Journal of Alloys and Compounds 502 (1) (2010) 147–152.

[18] Y.C. Chen, Y.N. Wang, C.H. Hsu, Elucidating the dielectric properties of $Mg_2SnO_4$ ceramics at microwave frequency, Journal of Alloys and Compounds 509 (2011) 9650–9653.

[19] Y.C. Chen, Microwave dielectric properties of $(Mg_{1-x}Co_x)_2SnO_4$ ceramics for application in dual-band inverted-E-shaped monopole antenna, IEEE Transactions on Ultrasonics, Ferroelectrics and Frequency Control 58 (2011) 2531–2538.

[20] W.W. Coffeen, Ceramic and dielectric properties of the stannates, Journal of the American Ceramic Society 36 (1953) 207–210.

[21] C. Wang, X.M. Wang, Synthesis, characterization and photocatalytic property of nano-sized $Zn_2SnO_4$, Journal of Materials Science 37 (2002) 2989–2996.

[22] B.W. Hakki, P.D. Coleman, A dielectric resonator method of measuring inductive in the millimeter range, IRE Transactions on Microwave Theory and Techniques MMT-8 (1960) 402.

[23] I. Stambolova, K. Konstantinov, D. Kovacheva, P. Peshev, T. Donchev, Spray pyrolysis preparation and humidity sensing characteristics of spinel zinc stannate thin films, Journal of Solid State Chemistry 128 (1997) 305–307.
[24] Y.H. Huang, J. He, Y. Zhang, et al., Morphology, structures and properties of ZnO nanobelts fabricated by Zn-powder evaporation without catalyst at low temperature, Journal of Materials Science 41 (10) (2006) 3057–3062.
[25] L.S. Wang, X.Z. Zhang, X. Liao, W.G. Yang, A simple method to synthesize single-crystalline $Zn_2SnO_4$ (ZTO) nanowires and their photoluminescence properties, Nanotechnology 16 (2005) 2928–2931.
[26] J.X. Wang, et al., Growth and characterization of axially periodic $Zn_2SnO_4$ (ZTO) nanostructures, Journal of Crystal Growth 267 (2004) 177–179.
[27] J.X. Wang, et al., Synthesis, structure and photoluminescence of $Zn_2SnO_4$ single-crystal nanobelts and nanorings, Solid State Communications 131 (2004) 435–437.
[28] X. Shen, J. Shen, S.J. You, L.X. Yang, et al., Phase transition of $Zn_2SnO_4$ nanowires under high pressure, Journal of Applied Physics 106 (2009) 113523–113525.
[29] Z.W. Wang, S.K. Saxena, In situ X-ray diffraction study of the pressure-induced transformation in nanocrystalline $CeO_2$, Solid State Communications 118 (2001) 75–78.
[30] J. Zeng, M. Xin, K. Li, et al., Transformation process and photocatalytic activities of synthesized $Zn_2SnO_4$ nanocrystals, Journal of Physical Chemistry C 112 (2008) 4159–4167.
[31] Z. Chen, M.H. Cao, C.W. Hu, Novel $Zn_2SnO_4$ hierarchical nanostructures and their gas sensing properties toward ethanol, Journal of Physical Chemistry C 115 (2011) 5522–5529.
[32] Y.P. Yuan, W.M. Du, X.F. Qian, $Zn_xGa_2O_{3+x}$ ($0 \le x \le 1$) solid solution nanocrystals: tunable composition and optical properties, Journal of Materials Chemistry 22 (2012) 653–659.
[33] Y.X. Lin, S. Lin, M.H. Luo, J.H. Liu, Enhanced visible light photocatalytic activity of $Zn_2SnO_4$ via sulfur anion-doping, Materials Letters 63 (2009) 1169–1171.
[34] R.D. Shannon, Dielectric polarizabilities of ions in oxides and fluorides, Journal of Applied Physics 73 (1) (1993) 348–365.
[35] W. Lei, W.Z. Lu, X.H. Wang, F. Liang, J. Wang, Phase composition and microwave dielectric properties of $ZnAl_2O_4$–$Co_2TiO_4$ low-permittivity ceramics with high quality factor, Journal of the American Ceramic Society 94 (1) (2011) 20–23.
[36] L. Colla, I.M. Reaney, N. Setter, Effect of structural changes in complex perovskites on the temperature coefficient of the relative permittivity, Journal of Applied Physics 74 (1993) 3414–3425.
[37] M.E. Song, J.S. Kim, M.R. Joung, S. Nahm, Synthesis and microwave dielectric properties of $MgSiO_3$ ceramics, Journal of the American Ceramic Society 91 (8) (2008) 2747–2750.
[38] M. Valant, D. Suvorov, Glass-free low-temperature cofired ceramics: calcium germinates, silicates and tellurates, Journal of the European Ceramic Society 24 (2004) 1715–1719.
[39] J.J. Xue, S.P. Wu, J.H. Li, Synthesis, microstructure and microwave dielectric properties of spinel $ZnGa_2O_4$ ceramics, Journal of the American Ceramic Society, http://dx.doi.org/10.1111/jace.12331.